Numerical Simulation and Analysis of Ocean Circulation of the Mediterranean outflow in the Gulf of Cadiz.

Léna Pitek

March 8, 2024

1 Introduction

The goal of this project was to conduct a numerical simulation of ocean circulation in a region of interest and analyze the results to gain insights into the dynamics and behavior of the ocean. For this project, the Western part of Gibraltar Strait in the Atlantic Ocean was selected due to its significance in the water exchange dynamics of Mediterranean waters outflowing through the Strait in the Atlantic. The simulation was conducted using the CROCO model, and the analysis focused on various aspects of ocean circulation, including surface kinetic energy, relative vorticity, temperature profiles, density, and velocity fields.

2 Model configuration

The simulation was set up using a realistic configuration of the Gulf of Cadiz. The resolution and size of the domain (30°N, 40°N, -20°E,-6°E) were chosen to ensure that the model could run correctly, considering a one-year spin up. The model setup considered factors such as horizontal resolution, time step, and domain size to ensure consistency with the dynamics of the region.

For my 1rst simulation : I used a spatial resolution of 1/8°, with a NTIMES of 40 000, a dt of 35 s and a Ndtfast of 850, over (30°N, 40°N ; -20°E,-6°E). From this we only get 1 year of initialization and 30 days of correct simulation.

Besides, I ran another simulation at the resolution of 1/3°, with a dt of 1800 s, NTIMES 35040, Ndtfast 60, over the same region, taking a bigger study area (20°N, 45°N ; -30°E, 0°E) in order to have a sufficient amout of timesteps to use. I will present the plots from the 1/3° simulation, and when useful or necessary rely on the 1/8 plots for a more specific analysis.

2.1 Largest Model Time Step

The largest model time step that could be used was determined based on the resolution and domain size. For 1/8° the time step was found to be dt = 41 s, which was obtained following the formula from CROCO tutorial $\Delta t \leq \frac{0.89\Delta x}{2\sqrt{gH}}$.

3 Results and Analysis

In order to manage the task of plotting at different timesteps and given my simulations, I was able to plot t = 10, 30, 90, 360 days for the 1/3° simulation and t = 10 and 30 days for the 1/8° simulation.

3.1 Time Evolution of Surface Kinetic Energy

The time evolution of surface kinetic energy integrated over the domain was analyzed for the simulation at 1/3°. The plot (Figure 1) shows a relatively constant kinetic energy varying around 1.2e10 J.

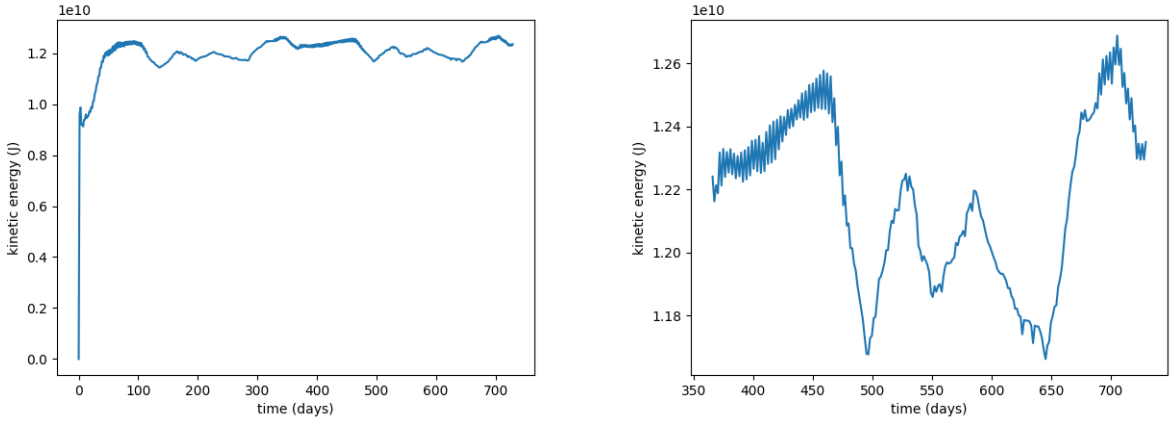

Figure 1: Time evolution of surface kinetic energy (KE) integrated over the domain for all timestep (left), for the year after one year initialization (right).

3.2 Snapshots of Relative Vorticity

We compute

$$\xi = -\frac{\partial u}{\partial y} + \frac{\partial v}{\partial x} \tag{1}$$

and divide by the f from the dataset with a for loop, and we get the following figures : careful to consider the day '0' being after 365 days of initialization of the simulation. Snapshots of relative vorticity normalized by the local Coriolis parameter were taken at different time intervals. Vorticity from the 1/3° simulation was not ideal to exploit and so is not presented here. Figure 2 (resp. Figure 3) shows snapshots of ζ/f at the surface (resp. at z = -400m) at t = 10, 30 days for the 1/8° simulation. These snapshots reveal vortices and shear zones: Vorticity normalized by the Coriolis parameter highlights regions of high vorticity (red) relative to the background rotation of the Earth. The contrasts are clearer at the surface than at z = 400m, but we can see the vorticity is conserved through depth. One point of interest will be the boundary current where vorticity is high in norm.

3.3 Snapshots of Temperature Profiles

Snapshots of temperature profiles at z = -400 m were analyzed at different time intervals. Figures 4a-4d show snapshots of temperature at z = -400 m at t = 10, 30, 90, 360 days with the 1/3° simulation, meanwhile Figures 4e and 4f show snapshots of temperature at z = -400 m at t = 10, 30 days with the 1/8° simulation. From Figures 4a-4d, we can see trends in temperatures at 400m depth : There is a clear delimitation between colder water in the north (about 11°C near the portuguese coasts) and warmer water (max of T of 14°C) in the south east of the area studied. On Figures 4e

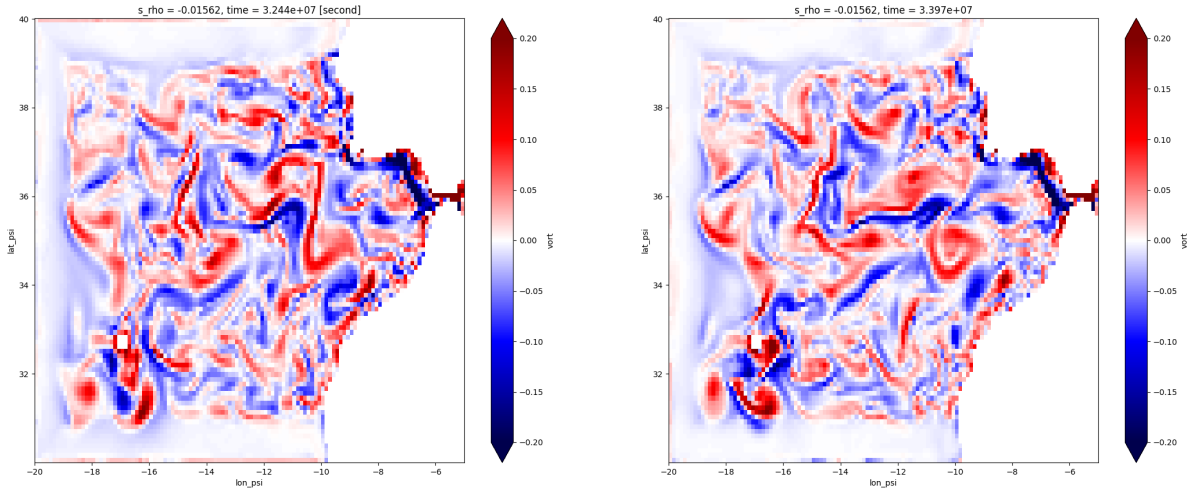

Figure 2: Snapshots of ζ/f (1/8°) at t=10 days (left), at t = 30 days (right) at the surface (last s_ρ level).

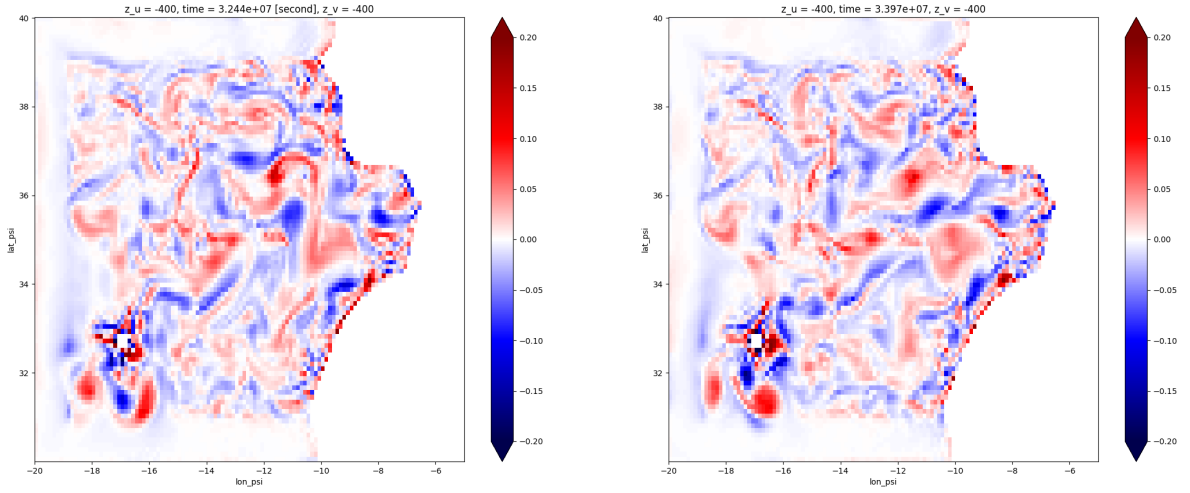

Figure 3: Snapshots of ζ/f (1/8°) at t=10 days (left), at t = 30 days (right) at z = -400 m.

and 4f we can get more insight on the temperature gradients in the Gulf of Cadiz, and the shape of the portuguese islands Madeira appears, the land/water mask being thiner. We can observe a cold tongue around the islands in the south west of the area (-17°E, 33°N). With these additional details we can discover the alternating cold and warm mesoscale structures that form the delimitation when

averaged in the axis of the strait at approximately 35°N. (see Figure 11 for comments on the realism on the simulations).

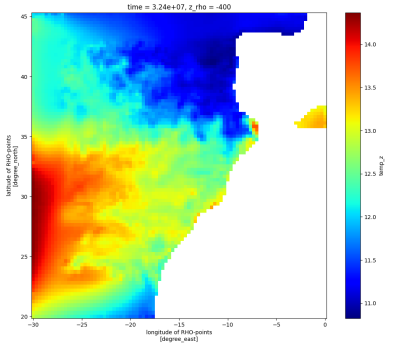

(a) Temperature at z = -400 m at t = 10 days

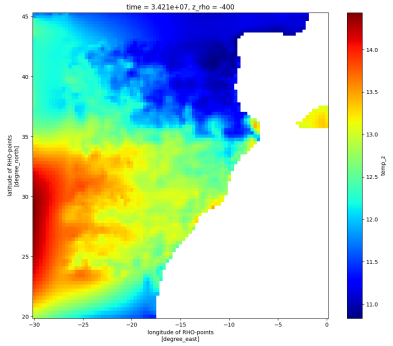

(b) Temperature at z = -400 m at t = 30 days

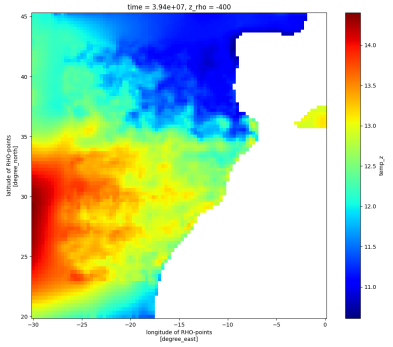

(c) Temperature at z = -400 m at t = 90 days

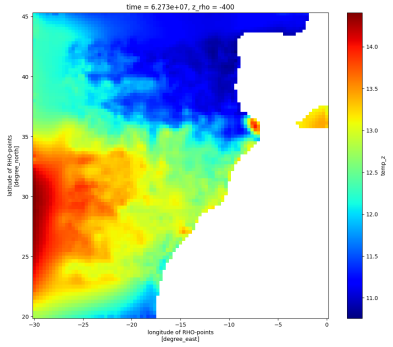

(d) Temperature at z = -400 m at t = 360 days

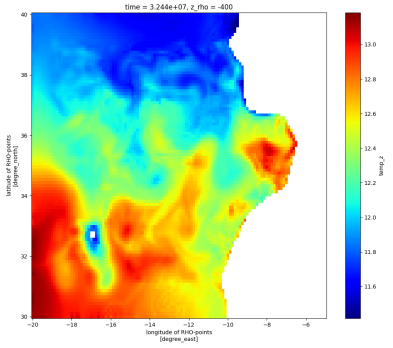

(e) Temperature at z = -400 m at t = 10 days

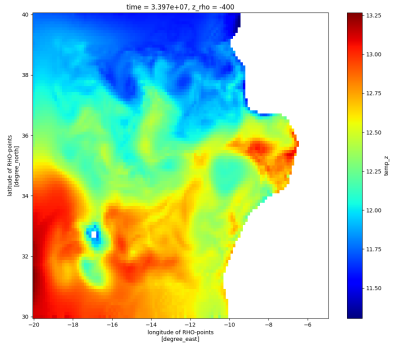

(f) Temperature at z = -400 m at t = 30 days

Figure 4: Snapshots of Temperature at z = -400 m : 1/3° at t = 10 (a), t = 30 (b), t = 90 (c) and t = 360 days (d) ; 1/8° at t = 10 (e), t = 30 (f).

3.4 Zonal or Meridional Sections of Density and Velocity

Meridional sections of density and velocity were analyzed at t = 10 for the 1/8° simulation. We compute density ρ thank to the gsw package and we choose to plot meridional vertical section along the Gibraltar Strait. Figure 5 (left) depicts the topography seamounts and as expected denser waters with increasing depth. In the right panel, the zonal section of u-velocity indicates velocities between $0 to 0.15 cm.s^{-1}$. Highest velocities in norm happen to be in blue, corresponding to the exit zone of Gibraltar Strait. This is also adding ot Figure 2, where the vorticity is more intense in norm in the area, and where the vein of current is flowing up the north coast of the Gulf of Cadiz.

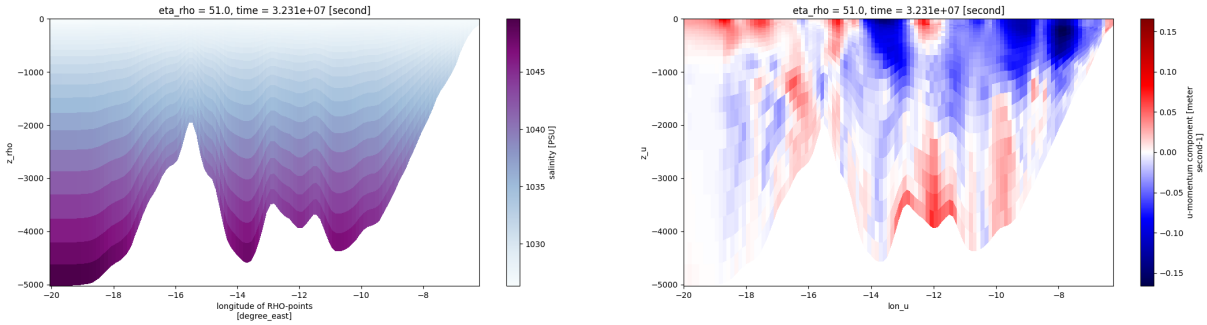

Figure 5: Vertical section of density (left) and zonal velocity (right) along the Gibraltar Strait. $\eta_\rho = 51$ corresponding to lat = 35.5, at t = 10 days (1/8°)

3.5 Mean Surface Velocities

The mean surface velocities over the last year of the simulation were computed and analyzed. The plot (Figure 6) illustrates the mean surface velocity patterns and significant trends. As intuited before from the vertical section of velocity, the maximal surface velocities are found to be at the exit of Gibraltar Strait.

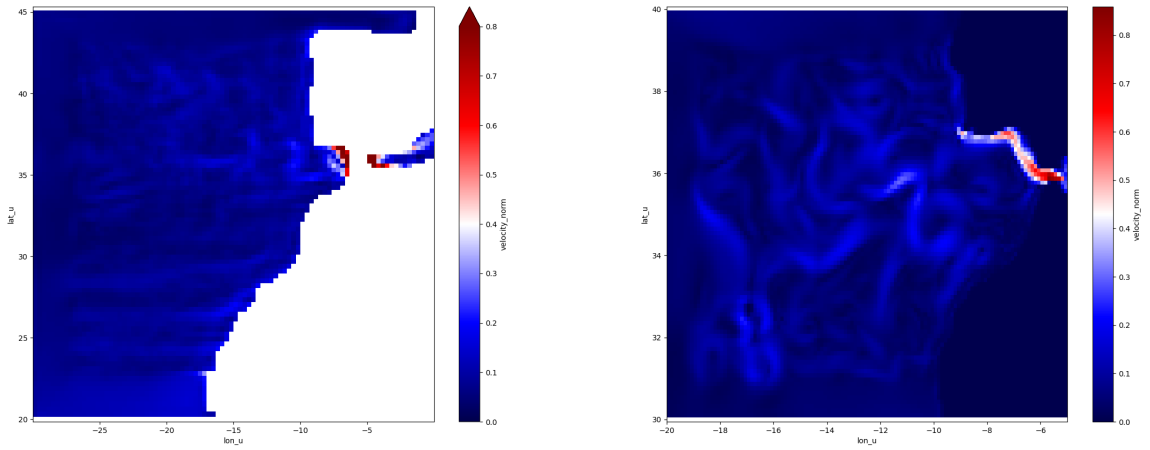

Figure 6: Mean Surface Velocities averaged over a year 1/3° (left) - averaged over 30 days, 1/8° (right)

3.6 Sea Surface Height

A map of sea surface height mean and variance over the last year of the simulation was generated using snapshots. The maps (Figures 7 and 8) provides insights into the spatial variability of sea surface height mean and variance for the two simulations

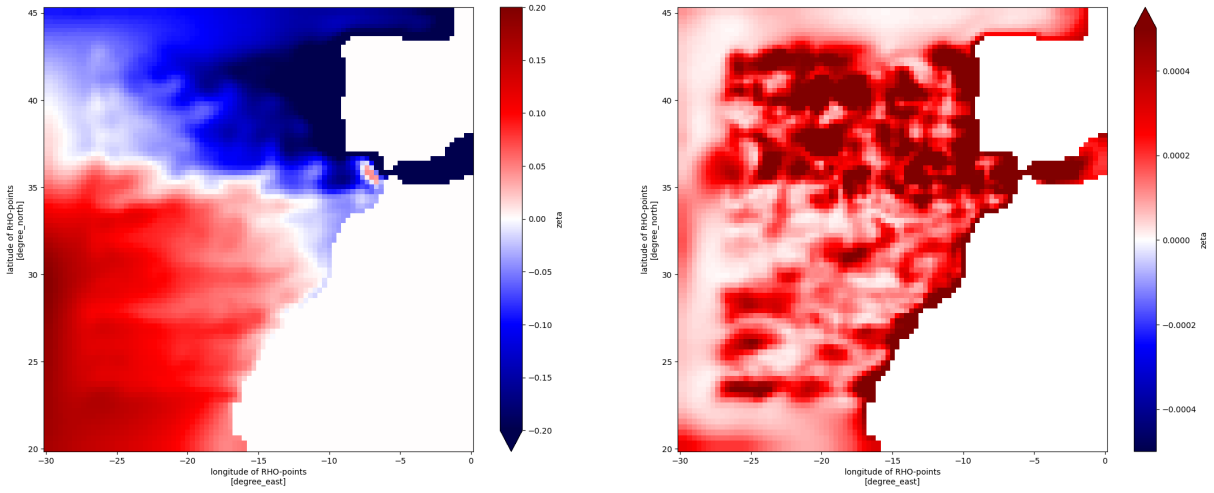

Figure 7: Map of SSH mean and variance over 1 year (1/3°)

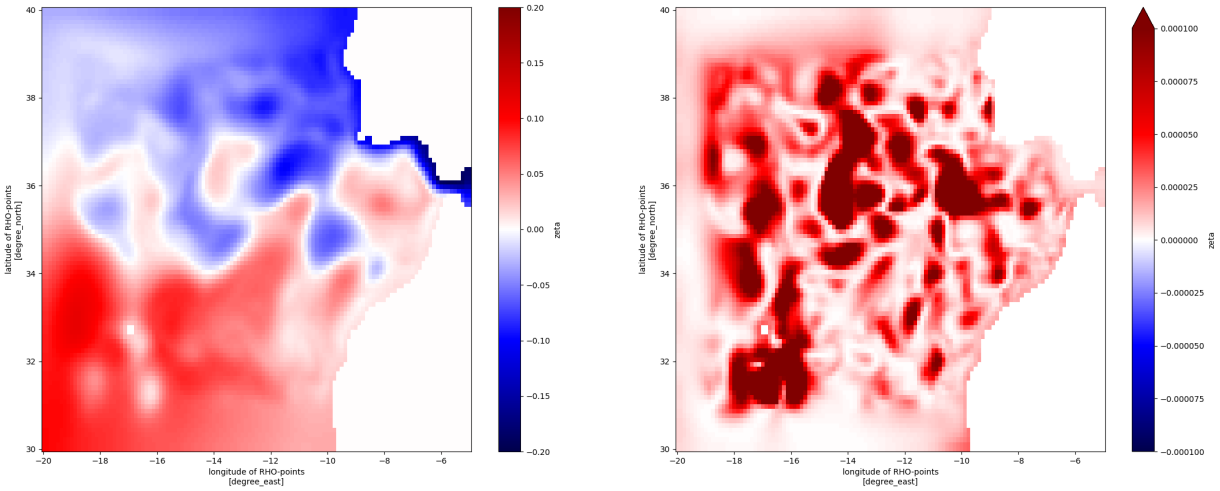

Figure 8: Map of SSH mean and variance over 30 days (1/8°)

On the left map of Figure 7, we can clearly sea a delimitation in sea surface height mean, north of the area being lower than south. On Figure 8, we can sea the vortices and meanders that forms this delimitation when averaged for a year. Variations in SSH are indicative of underlying ocean currents and fronts. In the left panel of Figure 8, we can see that regions of high SSH variance often coincide with areas of instabilities, such as baroclinic and barotropic instabilities. These instabilities arise from the interaction between different water masses, density gradients, and shear flows, leading to the generation of mesoscale features like eddies and meanders we highlighted on vorticity snapshots Figures 2 and 3.

3.7 Map of Surface Eddy Kinetic Energy

A map of surface eddy kinetic energy estimated over the last year of the simulation was obtained from the computed kinetic energy of question 2, to which we removed the temporal mean averaged over a year. First, the map (Figure 9) is consistent with previous observations on surface velocities, with the highest values following the north east coast near the strait.

Figure 9 also confirms what has been seen on SSH variance maps : high values of EKE indicate regions where eddies are particularly energetic and dynamic. The regions of enhanced mesoscale eddy activity are thus here concentrated along the Spanish coast, along the meanders and around the portuguese islands.

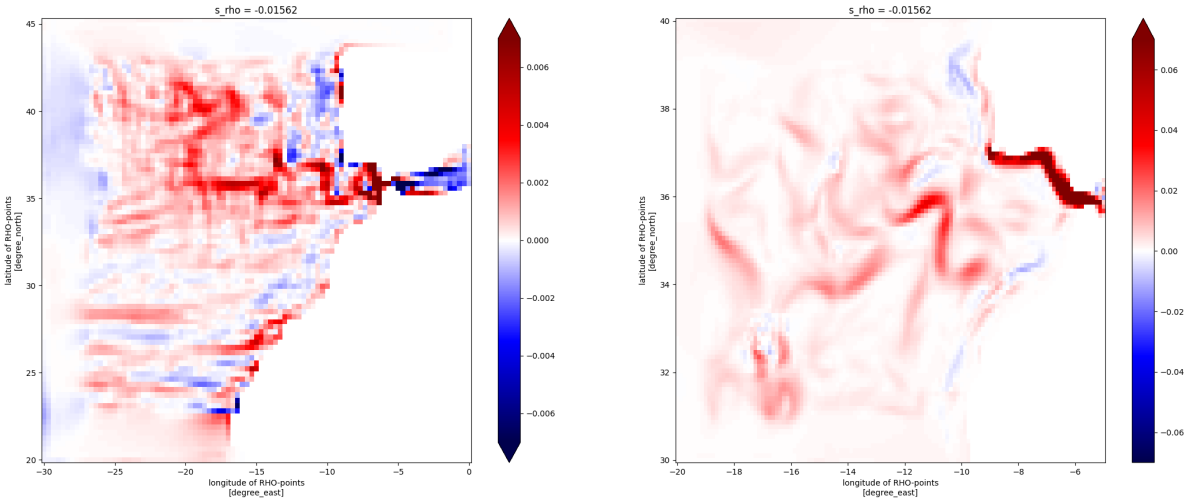

Figure 9: Map of surface EKE (eddy kinetic energy) estimated over the last year of the simulation (1/3°) and over 30 days (1/8°)

4 Conclusion on the realism of the simulation

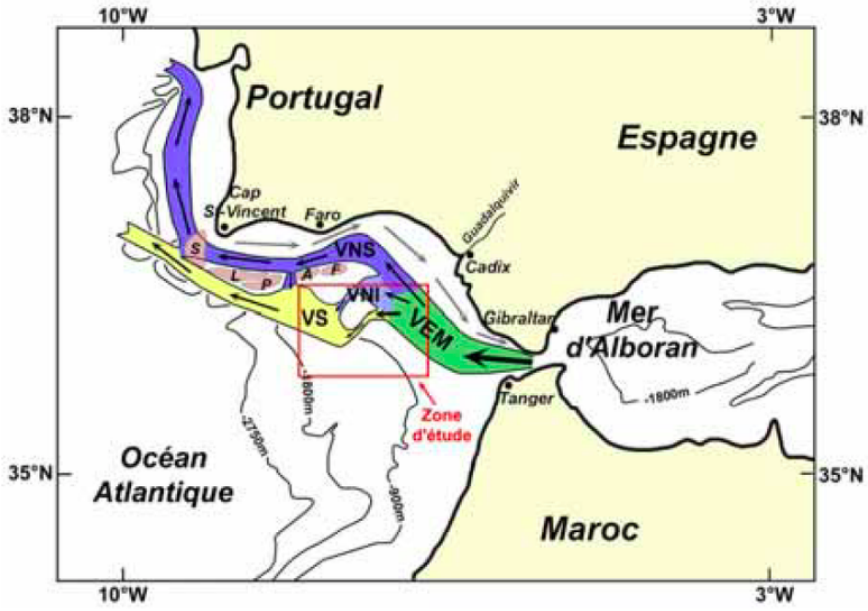

Figure 10: Description of the currents in the region from Hanquiez, n.d.

The comparison of our simulation results with the study by Molly O'Neil Baringer, 1997 on the physical oceanography of the Mediterranean Sea, particularly focusing on the Gulf of Cadiz, provides valuable insights into the realism of our model. Our analysis, as presented in Figures 2, 3, and 6, reveals the presence of realistic inertial currents and complex flow patterns influenced by underlying topography. These features closely resemble the expected behavior described by Molly O'Neil Baringer, 1997, indicating a high degree of fidelity in our simulation.

Furthermore, Figure 6 provides valuable insight into the entrainment of North Atlantic Central Water by the Mediterranean plume, consistent with the loss of density anomaly described by Molly O'Neil Baringer, 1997. The presence of westward transport of Mediterranean water, as highlighted in Figure 10, corroborates our observations from mean velocities averaged on 6. In order to get more insight on the separation of the Mediterranean water vein (VEM) into three smaller veins (VNS : North Superior Vein, VNI : North Intermediate Vein, VS : South Vein) further analysis should be done. Additional simulations should be considered when looking for mesoscale structures that have been studied by Carton, 2002 on Figure 14, in order to compare the vertical cross sections of temperature and salinity provided Figure 13, and thus add more realism to the simulations. It is also interesting to find that topography from the simulations and from WOA do not always coincide (see Figure 12) : at longitude of 12°W, the seamounts are clearly higher for WOA (right) than for our 1/8° simulation (left). Figure 11 affirms what is shown on 4 about temperature at a 400m depth. This alignment with established oceanographic phenomena further enhances the credibility of our simulation results.

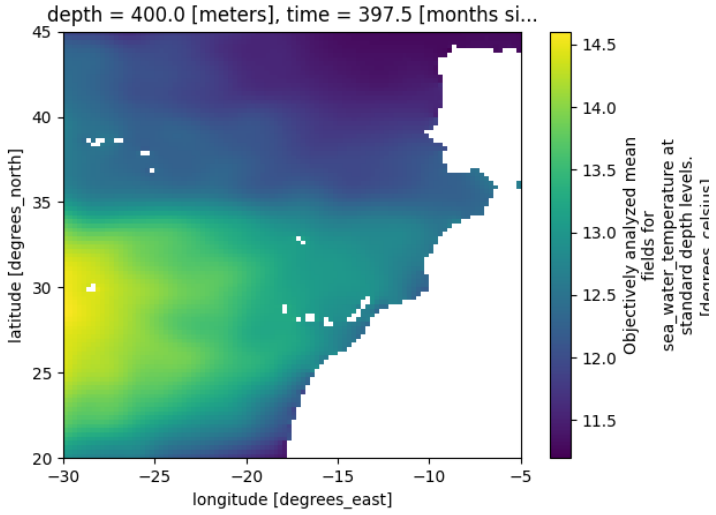

Figure 11: Temperature at 400m from WOA data (1/4°), averaged over time for the seasonal winter over all decades.

In addition, the salinity distribution depicted in the right panel of Figure 13 offers valuable information about the distribution of different water masses in the Gulf of Cadiz. These findings contribute to our understanding of the complex relationship between the Mediterranean Outflow Water (MOW), the Atlantic Meridional Overturning Circulation (AMOC), and climate variations in the North Atlantic.

It's worth noting that sedimentation in the middle slope of the Gulf of Cadiz, as strongly influ-

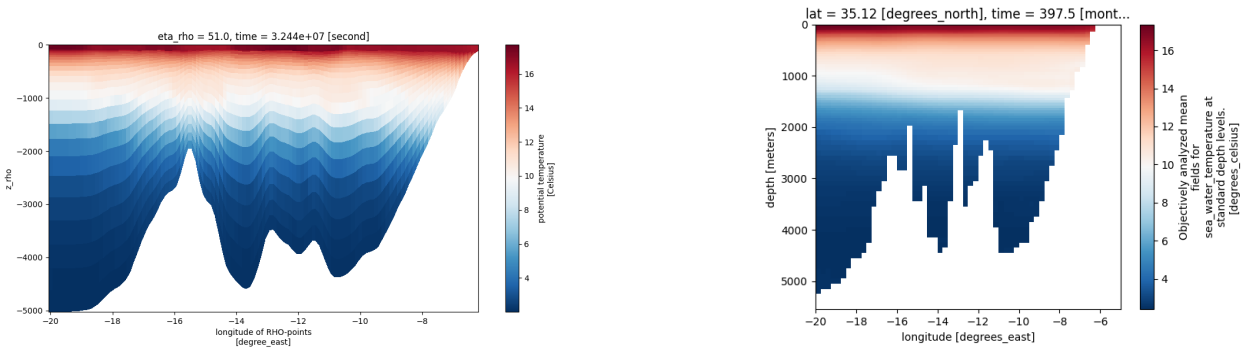

Figure 12: Vertical section of temperature from 1/8° simulation at t = 10 days (left), and from WOA data averaged over time for the seasonal winter (right).

enced by Mediterranean Outflow Water (MOW) Hanquiez, n.d., adds another layer of complexity to the region's oceanographic dynamics.

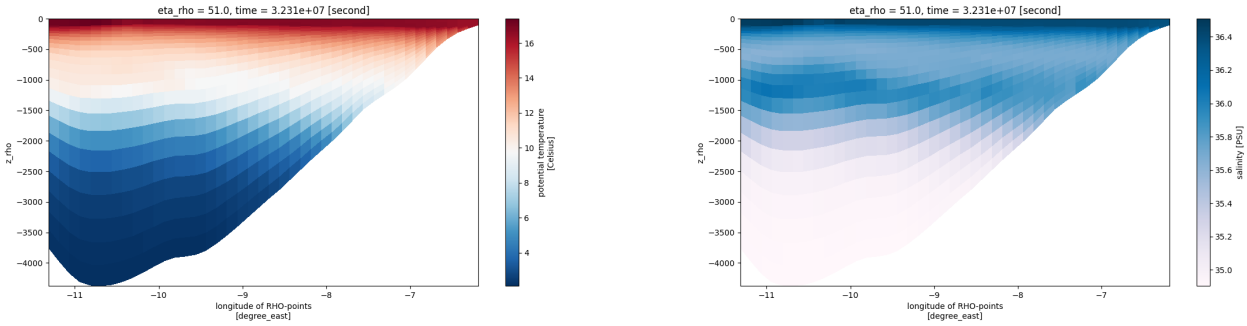

Figure 13: Vertical cross sections at t = 10 day of temperature (left) and salinity (right) along 35°N from 11°W to 6° W, comparable to Carton, 2002.

Overall, our simulation results demonstrate a high level of agreement with established oceanographic processes and phenomena described in the literature, affirming the realism and reliability of our model.

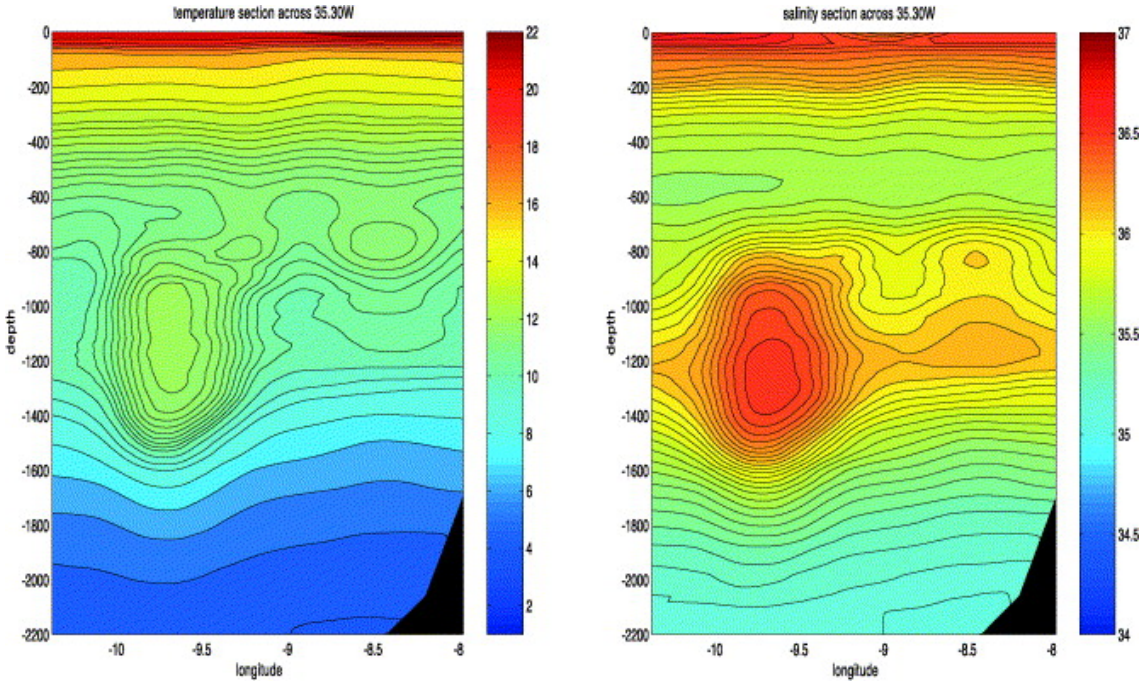

Figure 14: Vertical cross sections of temperature (left) and salinity (right) along 35°30'N from 10°25'W to 8° W, from Carton, 2002.

Bibliography

Carton, Xavier (2002). "Meddy coupling with a deep cyclone in the Gulf of Cadiz".

Hanquiez, V. (n.d.). "Analyse morphosédiementaire du Golfe de Cadiz" ().

Molly O'Neil Baringer, James F. Price (1997). "A review of the physical oceanography of the Mediterranean outflow".